$CpFe(CO)_2SnW_{11}PO_{39}^{4-}$. $CpFe(CO)_2SnCl_3$[10] (3.0 g, 7.5 mmol) in tetrahydrofuran (10 mL) was added to $Na_2WO_4 \cdot 2H_2O$ (15.0 g, 45.4 mmol) and $NaH_2PO_4 \cdot H_2O$ (3.0 g, 21.7 mmol) in water (50 mL). The mixture was heated to 60 °C; hydrochloric acid (12 M, 15 mL) was added dropwise, resulting in a temperature increase to 78 °C. The mixture was stirred 60 min at 60–78 °C and filtered hot. It was refiltered after cooling to room temperature. The addition of excess trimethylammonium chloride to the filtrate precipitated a solid, which was recrystallized from boiling water (100 mL) to obtain 1.5 g (11%) of $[(CH_3)_3NH]_4CpFe(CO)_2SnW_{11}PO_{39} \cdot 3H_2O$, identical by infrared analysis with that prepared earlier from $W_{11}PO_{39}^{7-}$ and $CpFe(CO)_2SnCl_3$.[4] Anal. Calcd for $[(CH_3)_3NH]_4C_5H_5Fe(CO)_2SnW_{11}PO_{39} \cdot 3H_2O$: C, 6.98; H, 1.57; N, 1.71; Fe, 1.71; Sn, 3.63. Found: C, 6.50; H, 1.43; N, 1.62; Fe, 1.42; Sn, 3.75.

NMR Spectra. ^{183}W NMR spectra were obtained on thermostated 20-mm diameter aqueous samples with use of a Nicolet NT360WB spectrometer at 15 MHz. ^{31}P spectra were obtained on the same instrument in 12-mm tubes at 146.1 MHz or on 10-mm samples in a CFT-80A at 32.2 MHz. ^{183}W chemical shifts were referenced to external 2 M Na_2WO_4 while ^{31}P chemical shifts are relative to external 85% H_3PO_4.

The spectrum shown in Figure 4A is the result of 10000 accumulations of 90° pulses (500 μs) with a recycle delay of 2.05 s. The 12 cm^3 of solution contained 18 g of $Li_7Ti_2W_{10}PO_{40}$. The FID was zero filled to 16K points and apodized with a 0.5-Hz exponential before Fourier transformation. The resolution-enhanced portion shown in Figure 5 was obtained by Gaussian–exponential double multiplication with use of standard Nicolet software.

The spectrum shown in Figure 4B is 26000 accumulations under the same conditions as above. Approximately 6 g of the salt was contained in 12 cm^3 of D_2O solution. The larger dispersion of resonances results in noticeable reduction of peak intensity toward the extremities because of the long (500-μs) pulses.

Acknowledgment. Fine technical assistance was given by G. A. Andrejack, M. P. Stepro, and G. Watunya.

Note Added in Proof. Since submission of this paper, several hardware improvements have allowed more sophisticated ^{183}W NMR experiments to be performed. A two-dimensional $^{183}W\{^{31}P\}$ INADEQUATE spectrum[12] of $Li_7[Ti_2W_{10}PO_{40}]$ has been obtained (Figure 6) and provides an unambiguous measure of the coupled sites without requiring accurate measurement of coupling patterns. Data are presented as a contour plot. Projection of the data onto the F_2 dimension (horizontal) shows a normal spectrum of pairwise ^{183}W–O–^{183}W isotopomers, while the second dimension (F_1, vertical) disperses those coupled peaks on the basis of the sum of the chemical shifts involved. The magnitudes of the couplings are retained so simple inspection of the contour pattern shows A coupled to B (edge), B to E (corner), E to C (edge), E to D (edge), C to A (corner), D to A (corner), and C to D (corner). The C–D edge connection is not observed, but both lines of the second-order C–D corner coupling are obvious.

Brevard and Schimpf[13] have also applied similar sophisticated two-dimensional methods to determining W–W connectivities in heteropolytungstates.

Registry No. $K_5MnTi_2W_{10}PO_{40}$, 84278-83-1; $K_5FeTi_2W_{10}PO_{40}$, 84278-84-2; $K_5CoTi_2W_{10}PO_{40}$, 84278-85-3; $K_5NiTi_2W_{10}PO_{40}$, 84278-86-4; $K_5CuTi_2W_{10}PO_{40}$, 84278-87-5; $K_5ZnTi_2W_{10}PO_{40}$, 84278-88-6; $Li_7Ti_2W_{10}PO_{40}$, 84278-89-7; $Cs_7Ti_2W_{10}PO_{40}$, 84303-03-7; $[(CH_3)_4N]_7Ti_2W_{10}PO_{40}$, 84303-05-9; $K_7Ti_2W_{10}PO_{40}$, 84303-06-0; $Cs_4KH_2Ti_2W_{10}PO_{40}$, 84303-07-1; $[(CH_3)_4N]_5CuTi_2W_{10}PO_{40}$, 84303-08-2; $K_5[CpFe(CO)_2Sn]_2W_{10}PO_{38}$, 84253-84-9; $[(CH_3)_3NH]_5[C_5H_5Fe(CO)_2Sn]_2W_{10}PO_{38}$, 84253-86-1; $(NH_4)_5[C_5H_5Fe(CO)_2Sn]_2W_{10}PO_{38}$, 84253-87-2; $Li_5[C_5H_5Fe(CO)_2Sn]_2W_{10}PO_{38}$, 84253-88-3; $[(CH_3)_3NH]_4CpFe(CO)_2SnW_{11}PO_{39}$, 84303-10-6.

(12) Mareci, T. H.; Freeman, R. *J. Magn. Reson.* **1982**, *48*, 158–163.
(13) Brevard, C.; Schimpf, P., submitted for publication in *J. Am. Chem. Soc.* (paper presented at the NATO Advanced Study Institute on Multinuclear NMR, Stirling, Scotland, Sept 1982).

Contribution from the Departments of Chemistry, The University of Texas, Austin, Texas 78712, and York University, Downsview, Ontario, Canada M3J 1P3

Electrogenerated Chemiluminescence. 42. Electrochemistry and Electrogenerated Chemiluminescence of the Tris(2,2′-bipyrazine)ruthenium(II) System

JAIME GONZALES-VELASCO,[1a,c] ISRAEL RUBINSTEIN,[1a] R. J. CRUTCHLEY,[1b] A. B. P. LEVER,[1b] and ALLEN J. BARD*[1a]

Received April 12, 1982

The electrochemical behavior and electrogenerated chemiluminescence (ecl) of $Ru(bpz)_3^{2+}$ (as the PF_6^- salt) in acetonitrile solutions were investigated. Oxidation to the 3+ form and reduction to the 1+, 0, 1−, and 2− forms occur at potentials about 0.5 V more positive than those for the corresponding bipyridine complex. Emission characteristic of $Ru(bpz)_3^{2+*}$ is produced upon the electron-transfer reaction between the 3+ and 1+ species. Weak emission also results from the reaction of the 3+ species with solvent or impurities.

Introduction

Of the numerous compounds that produce chemiluminescence upon the electron-transfer reactions of electrogenerated species (ecl), that observed with the $Ru(bpy)_3^{2+}$ (bpy = 2,2′-bipyridine) system is among the most intense and best characterized.[2-4] A recent report[5] of a new, related compound, $Ru(bpz)_3^{2+}$ (bpz = 2,2′-bipyrazine)

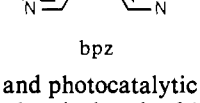

bpz

and its spectroscopic and photocatalytic properties suggested a study of the electrochemical and ecl behavior of this compound. Previous studies of $Ru(bpy)_3^{2+}$ showed that ecl is produced by the redox reaction between the 1+ and 3+ species as well as by reaction of the 3+ species with a number of reductants (e.g., especially oxalate).[2d] We were particularly interested in $Ru(bpz)_3^{2+}$ because the redox processes are shifted by ~0.5 V toward more positive potentials, compared with those for $Ru(bpy)_3^{2+}$. This could prove valuable in ecl in aqueous media where proton reduction interferes at negative potentials. A comparison of the ecl efficiency between the bpz

(1) (a) The University of Texas. (b) York University. (c) Permanent address: Faculty de Ciencias, Universite Autonoma de Madrid, Cuidad Universite de Canto Blanco, Madrid 34, Spain.
(2) (a) Tokel, N. E.; Bard, A. J. *J. Am. Chem. Soc.* **1972**, *94*, 2862. (b) Tokel-Takvoryan, N. E.; Hemingway, R. E.; Bard, A. J. *Ibid.* **1973**, *95*, 6582. (c) Wallace, W. L.; Bard, A. J. *J. Phys. Chem.* **1979**, *83*, 1350. (d) Rubinstein, I.; Bard, A. J. *J. Am. Chem. Soc.* **1981**, *103*, 512–516. (e) Luttmer, J. D.; Bard, A. J. *J. Phys. Chem.* **1981**, *85*, 1155–1159.
(3) Glass, R. S.; Faulkner, L. R. *J. Phys. Chem.* **1981**, *85*, 1159.
(4) Itoh, K.; Honda, K. *Chem. Lett.* **1979**, 99.
(5) (a) Crutchley, R. J.; Lever, A. B. P. *J. Am. Chem. Soc.* **1980**, *102*, 7128. (b) Crutchley, R. J.; Lever, A. B. P. *Inorg. Chem.* **1982**, *21*, 2276.

0020-1669/83/1322-0822$01.50/0 © 1983 American Chemical Society

and bpy complexes is also of interest.

In this paper we describe the electrochemical behavior of the $Ru(bpz)_3^{2+}$ system in acetonitrile (MeCN) solutions and demonstrate the production of ecl and its characteristics.

Experimental Section

Chemicals. $Ru(bpz)_3^{2+}$ was obtained in the form of the PF_6^- salt.[5] It was recrystallized from MeCN and dried for 25 h under vacuum at room temperature. The tetra-*n*-butylammonium hexafluorophosphate (TBAFP) used as supporting electrolyte was prepared by the reaction of NH_4PF_6 (Ozark-Mahoning) and tetra-*n*-butylammonium perchlorate (Aldrich). The precipitate of TBAFP obtained was filtered and repeatedly washed with distilled water. The precipitate was dissolved in boiling EtOH; when the solution was cooled, TBAFP was obtained in the form of small crystals. This procedure was repeated three times. Finally the crystals were recrystallized from a mixture of acetone and ether and dried under a vacuum.

Spectroquality grade acetonitrile (MCB) was degassed by freeze–pump–thaw cycles ($<10^{-5}$ torr). A MeCN/0.1 M TBAFP solution did not show appreciable Faradaic currents at a Pt electrode between −2.6 and +2.5 V vs. the Ag-wire quasi reference electrode (AgRE).

Apparatus. A Princeton Applied Research (PAR) Model 173 potentiostat and a PAR Model 175 universal programmer were used for voltammetric experiments. The output of the PAR Model 176 current follower was recorded directly with a Houston Instruments Model 2000 X-Y recorder. The coulometric experiments employed a PAR 179 digital coulometer.

Procedure. The test solutions were prepared under He in a Vacuum Atmospheres glovebox equipped with a Model MO 40-1 Dri-Train. Electrochemical and ecl experiments were carried out in a three-compartment working cell with a volume of 3 cm^3. The working electrode compartment was provided with an optically flat Pyrex glass window of area approximately 2 cm^2, and the working electrode, a polished platinum disk of area 0.06 cm^2, was aligned parallel to the window. The distance between the working electrode and the window was around 3 mm. The counterelectrode was a platinum foil, of area $\simeq$3 cm^2. A silver wire immersed in the MeCN/TBAFP solution and separated from the working electrode chamber by a medium-porosity frit was used as a quasi reference electrode (AgRE). The potential of this Ag-wire electrode was measured against an aqueous calomel electrode (SCE) and checked vs. the ferrocene/ferrocenium couple in MeCN and was found to have a potential of +0.055 V vs. SCE.

The ecl measurements were carried out after transferring the sealed working cell to a light-tight box whose interior was painted with black nonreflective paint. The emitted light was measured with a Hamamatsu TV Corp. R928 photomultiplier tube. The ecl spectrum was taken by using an Oriel Co. monochromator. Emission and absorption spectra were obtained with an Aminco-Bowman spectrophotofluorometer (SPF) without slits for ecl studies and a Cary Model 14 UV and visible spectrophotometer, respectively.

Results and Discussion

Electrochemical Results. A typical cyclic voltammogram (CV) for 1 mM $Ru(bpz)_3^{2+}$ in MeCN/0.1 M TBAFP is shown in Figure 1. The peak potentials for the oxidation (E_{pa}) and reduction (E_{pc}) waves and ΔE_p values for each wave are given in Table I. The general electrochemical behavior of the $Ru(bpz)_3^{2+}$ system is very similar to that of $Ru(bpy)_3^{2+}$ in MeCN, but there are significant differences. The reductions to the 1+, 0, and 1− species and the oxidation to the 3+ species occur with all peaks shifted 0.5 V toward more positive potentials as compared to those for the bpy complex. Thus the $Ru(bpz)_3^{3+}$ species is a significantly stronger oxidant than is $Ru(bpy)_3^{3+}$, and its production from the 2+ form occurs much nearer to the anodic limit of the MeCN/TBAFP solution. Because of this, $Ru(bpz)_3^{3+}$ is less stable than the bpy complex in this medium, which leads to differences in the characteristics of the 3+/2+ wave and the ecl. On the other hand, the fourth reduction wave (marked V in Figure 1) shows a well-defined reversal peak at a scan rate, v, of 100 mV/s at room temperature, indicating some stability of the 2− species. No such stability is observed with the corresponding bpy form that is produced at a potential about 0.5 V more negative. Only at

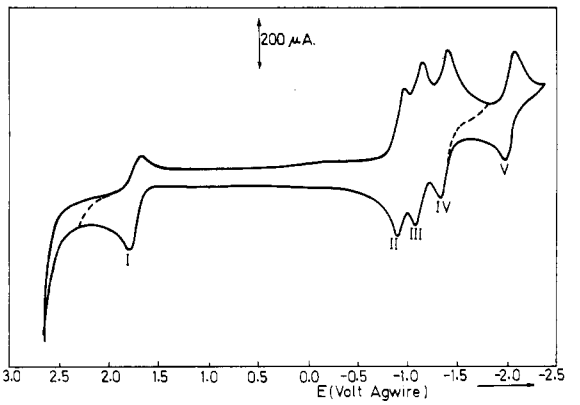

Figure 1. Cyclic voltammogram of 1 mM $Ru(bpz)_3^{2+}(PF_6^-)_2$/MeCN/0.1 M TBAFP at a Pt electrode (scan rate 100 mV/s, T = 25 °C, Ag-wire reference electrode).

Table I. Cyclic Voltammetric Peak Potentials (E_p) for $Ru(bpz)_3^{2+}$ in 0.1 M TBAPF/Acetonitrile Solutions at a Platinum Electrode (T = 25 °C)[a]

	peaks in Figure 1				
	I	II	III	IV	V
E_{pc}(redn), V vs. AgRE	+1.85	−0.800	−0.980	−1.250	−2.075
E_{pa}(oxidn), V vs. AgRE	+1.94	−0.730	−0.910	−1.180	−1.975
no. of electrons	1	1	1	1	1
ΔE_p(25 °C, 100 mV/s), V	90	70	70	70	100
redox states	3+/2+	2+/1+	1+/0	0/1−	1−/2−

[a] Potential values were measured against an Ag-wire quasi reference electrode in the same solution. The Ag wire showed a potential of +55 mV measured against a SCE in the same solution.

v > 20 V/s or at temperatures of −30 °C was any reversal anodic peak seen for the corresponding bpy wave.[2] However, repeated scanning over wave V to produce the reduced 2− form led to the formation of a deep brown solution caused by decomposition of this species. Moreover, the rest potential of this solution after this cycling was −0.2 V vs. AgRE as compared to the initial value of about +0.54 V, indicating irreversible production of a reduced species. The resulting brown solution could not be electrochemically oxidized back to the original orange $Ru(bpz)_3^{2+}$ solution. Similar, but slower, decomposition occurred upon scanning or holding the potential at values corresponding to peaks III and IV (Figure 1).

The one-electron nature of the waves was confirmed by controlled-potential coulometry (CPC) measurements. Reduction at −0.8 vs. AgRE near the peak of the first reduction wave (wave, II, Figure 1) gave an n_{app} value (corresponding to number of faradays per mole) of 0.98. Oxidation of the reduced solution back to the 2+ form showed $Q_b/Q_f \simeq 0.9$ (where Q_f and Q_b are the number of coulombs consumed during the forward reduction and reverse oxidation, respectively)[6a] for an experimental duration of ~1 h. This demonstrates the relatively high stability of the 1+ species.

Cyclic voltammetric data for the reduction waves (II–IV) shown in Figure 1 are contained in Table II. Because of the close spacing of the reduction waves, it was difficult to determine precise values for peak currents (i_{pc} and i_{pa}) and potentials. However, the current functions ($i_{pc}/v^{1/2}C$) for all three waves are about the same, demonstrating that all three are one-electron transfers. Moreover, the values of $i_{pa}/i_{pc} \simeq 1$ for these waves demonstrate that the 1+, 0, and 1− forms are stable on the CV time scale.

(6) Bard, A. J.; Faulkner, L. R. "Electrochemical Methods"; Wiley: New York, 1980: (a) p 479; (b) p 455.

Table II. Cyclic Voltammetric Results for the Three Reductions of $Ru(bpz)_3^{2+}$ [a]

	peak II			peak III			peak IV		
ν, mV/s	ΔE_p, mV	i_{pa}/i_{pc}	$i_{pc}/\nu^{1/2}C$	ΔE_p, mV	i_{pa}/i_{pc}	$i_{pc}/\nu^{1/2}C$	ΔE_p, mV	i_{pa}/i_{pc}	$i_{pc}/\nu^{1/2}C$
10	30	1.00	1.2	60	1.00	1.4	70	0.88	1.2
20	60	1.40	1.0	60	0.97	1.6	60	0.88	1.3
50	60	1.00	1.0	60	1.28	1.2	70	0.90	1.4
100	60	1.11	0.9	80	1.00	1.7	70	0.83	1.7
200	70	1.45	0.6	80	1.03	1.2	90	0.75	1.6
500	90	1.28	0.6	80	0.95	1.3	80	0.70	1.4
1000	100	1.45	0.7	100	1.12	1.5	110	0.68	1.9

[a] The solution was 1.0 mM $Ru(bpz)_3^{2+}(PF_6^-)_2$ and 0.1 M TBAFP in CH_3CN at 25 °C. $\Delta E_p = E_{pc} - E_{pa}$; C = concentration of complex. Peak currents for waves III and IV were measured from the extrapolated decreasing current of the preceding wave. The units for the current function evaluation were i, A/cm²; $\nu^{1/2}$, $(V/s)^{1/2}$; C, M.

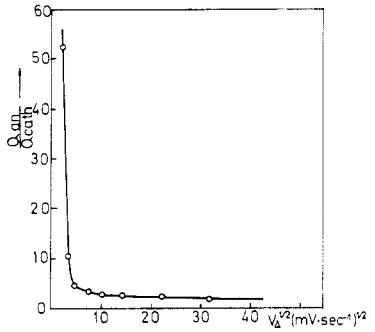

Figure 2. Ratio between the anodic and cathodic charges in wave I as a function of the scan rate (T = 25 °C). The solution is the same as in Figure 1.

For wave II the value of i_{pa}/i_{pc} is significantly larger than 1; this suggests that some deposition or adsorption of the 1+ species occurs on the electrode. Although the CV data show stability of the 0 and 1− forms on the short time scale, repeated cycling through these waves causes some color change in the solution as well as the formation of a deposit on the electrode surface.

As for wave I, corresponding to the 3+/2+ oxidation–reduction process, the potential for this wave is close to the anodic stability limit of Pt in MeCN and the $Ru(bpz)_3^{3+}$ species reacts with a component in the MeCN/TBAFP medium to regenerate the 2+ species, giving rise to a catalytic wave.[6b] The CV parameters for wave I confirm the catalytic nature of this wave. For example, as shown in Figure 2, the ratio of peak heights, i_{pa}/i_{pc}, or peak areas, Q_a/Q_c, increases sharply with decreasing v. At low scan rates the ratio Q_a/Q_c is very high since the 2+ species is continuously regenerated during the scan. At higher scan rates the ratio approaches unity because no appreciable reaction of the 3+ form occurs at short times.

A voltammogram taken after repeated application of pulses between −0.8 and +1.9 V vs. AgRE (the range for ecl, as described below), as shown in Figure 3, suggests decomposition of the $Ru(bpz)_3^{2+}$ complex since new peaks at +1.5 V vs. AgRE near wave I and at −0.4 vs. AgRE before wave II appear. The new anodic peak at +1.5 V appears after a cathodic scan to −1.2 V, and the new cathodic peak at −0.4 appears after a scan to +2.2 V. The species giving rise to these waves is not known.

After these repeated pulsing experiments, the electrode surface was covered with a yellowish-brown precipitate. Although the nature of this precipitate was not elucidated, it probably can be attributed to the formation of reduced Ru species. The decomposition process is enhanced when the cathodic scan limit is more negative.

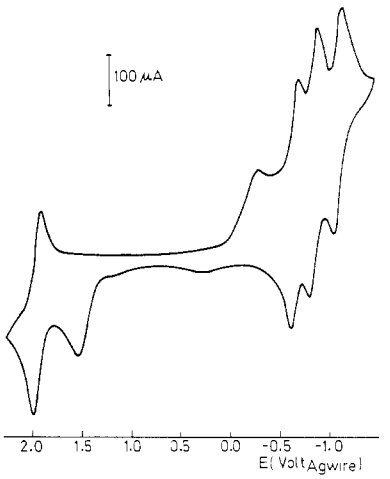

Figure 3. Cyclic voltammogram of 1 mM $Ru(bpz)_3(PF_6)_2$/MeCN/0.1 M TBAFP after repeated pulsing between −0.8 and +1.9 V vs. AgRE.

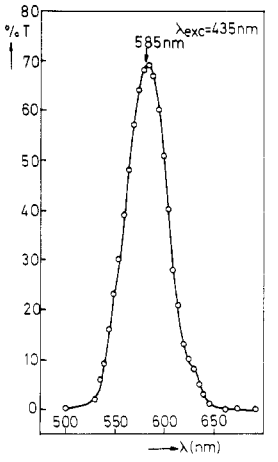

Figure 4. Luminescence spectrum of a 10^{-5} M solution of $Ru(bpz)_3^{2+}$ in MeCN at room temperature.

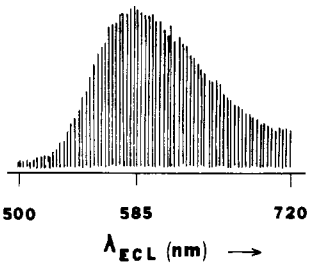

Figure 5. Ecl spectrum of a 1 mM $Ru(bpz)_3(PF_6)_2$/MeCN/0.1 M TBAFP solution (pulsing limits −0.8 and +1.85 V vs. AgRE at 0.5 Hz).

Emission Spectrum of $Ru(bpz)_3^{2+}$. The emission spectrum of a 10^{-5} M solution of $Ru(bpz)_3^{2+}$ in MeCN at room temperature is shown in Figure 4. An excitation wavelength for maximum absorption (435 nm) leads to the emission maximum at 585 nm for the luminescence of the sample. This wavelength is 25 nm shorter than the emission maximum of $Ru(bpy)_3^{2+}$.

Ecl spectrum of $Ru(bpz)_3^{2+}$ in Acetonitrile. By pulsing of the potential applied to the platinum electrode between 1.95 and −0.85 V vs. AgRE an orange ecl emission was observed. The light intensity obtained was lower than that for $Ru(bpy)_3^{2+}$ under equivalent conditions and decayed more rapidly. The ecl spectrum of $Ru(bpz)_3^{2+}$ (Figure 5) shows an emission maximum at 585 nm, identical with the emission spectrum obtained on photoexcitation. These results are similar to those obtained with $Ru(bpy)_3^{2+}$. The mechanism for emission is

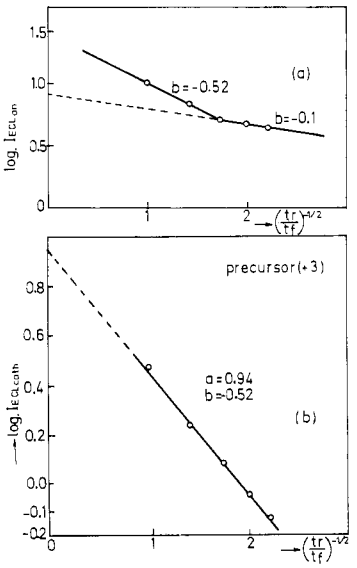

Figure 6. Feldberg–Faulkner plots for the solution in Figure 1: (a) precursor $Ru(bpz)_3^+$; (b) precursor $Ru(bpz)_3^{3+}$.

probably the same in both cases, namely, reaction of the 3+ and 1+ forms to yield the 2+ excited state (eq 1–3). This

$$Ru(bpz)_3^{2+} + e^- \rightleftharpoons Ru(bpz)_3^+ \quad (1)$$

$$Ru(bpz)_3^{2+} - e^- \rightleftharpoons Ru(bpz)_3^{3+} \quad (2)$$

$$Ru(bpz)_3^{3+} + Ru(bpz)_3^+ \rightarrow Ru(bpz)_3^{2+*} + Ru(bpz)_3^{2+} \quad (3)$$

homogeneous redox reaction has a free energy of −2.7 eV (as calculated from the E_p values of the 3+/2+ and 2+/1+ and waves, with the assumption of an entropic contribution of 0.1 eV).[7] This is greater than the energy of the emitting charge-transfer state, 2.12 eV. The singlet excited state for $Ru(bpz)_3^{2+}$ occurs at 2.85 eV[8] so that direct population of this state does not appear possible, and direct formation of the emitting triplet is proposed. This is analogous to the results in the $Ru(bpy)_3^{2+}$ system.[2-4]

Characteristics of the Ecl. Recent studies[2e,3] of the ecl intensity $(t_r/t_f)^{1/2}$ behavior (where t_f is the forward pulse time and t_r the reverse pulse time) for the $Ru(bpy)_3^{2+}$ system at short times ($(t_r/t_f)^{-1/2} = 1-10$) showed that these Feldberg–Faulkner plots[9,10] corresponded closely to that expected of an "S-route" system, where direct population of the emitting state on electron transfer occurs. Similar plots for the $Ru(bpz)_3^{2+}$ system are shown in Figure 6. When either the 1+ (Figure 6a) or the 3+ (Figure 6b) form is generated first, the behavior is very different from that of the theoretical model, which predicts a slope of −1.42. The cause for this deviation is probably the instability of the 3+ form and perhaps quenching by decomposition products. This nonideal behavior is also apparent from the ecl intensity–time transient itself (Figure 7). The anodic transient (following production of the 1+ species) shows a peak that decays to an almost steady value. This attainment of a steady value is also apparent from the change in slope in the plot of Figure 6a. The following cathodic transient is very sharp and decays rapdily to background. The steady level of emission during the anodic pulse

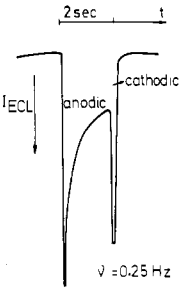

Figure 7. Typical ecl intensity–time transient (I_{ecl} in arbitrary units, T = 25 °C). The solution is the same as in Figure 1.

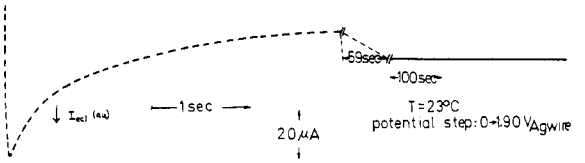

Figure 8. Ecl intensity–time transient obtained by pulsing between −0.85 and +1.9 V vs. AgRE for 3 s and holding the potential at +1.9 V. The solution is the same as in Figure 1.

represents a reaction of the 3+ species with solvent, electrolyte, or impurities to produce emission. That this is clearly the case can be seen from the anodic transient in Figure 8, where the potential was maintained at +1.90 V and a constant weak emission was observed. Recent studies have shown that the reaction of $Ru(bpy)_3^{3+}$ with oxalate, organic acids, or other reductants results in emission,[2d,11,12] so a similar reaction by the stronger oxidant $Ru(bpz)_3^{3+}$ appears reasonable. Thus the anodic step involves the 1+/3+ electron-transfer reaction as well as the 3+/background emission. During the subsequent cathodic step the 3+ species has been depleted by this background reaction and less is available to react with the generated 1+ species, producing the rapid decay of intensity.

Conclusions

The electrochemical behavior of the $Ru(bpz)_3^{2+}$ system generally parallels that of the corresponding bpy system, but the peaks are shifted by about 0.5 V toward more positive potentials. Since the 2+/3+ wave is best represented by electron transfers involving metal centers, the shift must be ascribed to greater stabilization of the 2+ vs. the 3+ form by the bpz. The reduction waves, e.g., the 2+/1+ wave, are better represented as reduction of the ligands, and the shift here represents easier reduction of bpz to the Ru^{2+} stabilized bpz^- species compared to that for bpy. The positive potential shift results in the 3+ bpz species being less stable in MeCN than the corresponding bpy species. Ecl reactions involving the 3+/1+ electron-transfer annihilation reaction and a reaction of the 3+ species with solvent or impurity to produce the $Ru(bpz)_3^{2+}$ excited states occur. There is precedence for both of these in the bpy system.

Acknowledgment. The support of this research by the Office of Naval Research (Grant No. N00014-78-C-0592) and the Army Research Office (Grant No. DAAG 29-82-K-0006) is gratefully acknowledged. J.G.-V. is grateful to the Comitê Hispano-Norteamericano de Cooperacion Cientifica y Tecnicâ for a grant.

Registry No. $Ru(bpz)_3^{2+}(PF_6^-)_2$, 80907-56-8; $Ru(bpz)_3^{3+}$, 84303-43-5; $Ru(bpz)_3^+$, 75523-97-6; $Ru(bpz)_3$, 75523-95-4; $Ru(bpz)_3^-$, 75523-94-3; $Ru(bpz)_3^{2-}$, 84303-44-6.

(7) Faulkner, L. R.; Tachikawa, H.; Bard, A. J. *J. Am. Chem. Soc.* **1972**, *94*, 691.
(8) Klassen, D. M.; Crosby, G. A. *J. Phys. Chem.* **1968**, *48*, 1853.
(9) Feldberg, S. W. *J. Phys. Chem.* **1966**, *70*, 3928.
(10) (a) Faulkner, L. R. *J. Electrochem. Soc.* **1977**, *124*, 1724. (b) *Ibid.* **1975**, *122*, 1190.
(11) Chang, M. M.; Saji, T.; Bard, A. J. *J. Am. Chem. Soc.* **1977**, *99*, 5399–5403.
(12) (a) Lytle, F. H.; Hercules, D. M. *Photochem. Photobiol.* **1971**, *13*, 123. (b) Monidez, W. K.; Leyden, D. E. *Anal. Chim. Acta* **1978**, *96*, 401.